Scientia Iranica B (2014) 21(1), 181–191

Sharif University of Technology
Scientia Iranica
Transactions B: Mechanical Engineering
www.scientiairanica.com

Machining command generation with a rotational C^2 PH quintic curve interpolant for cam profile manufacturing

J. Jahanpour* **and H. Dolatabadi**

Department of Mechanical Engineering, Mashhad Branch, Islamic Azad University, Mashhad, P.O. Box: 9187147578, Iran.

Received 2 May 2012; received in revised form 2 August 2013; accepted 21 August 13

KEYWORDS
Cam profile;
C^2 PH quintic curve;
Junction point;
Rotational interpolation;
CNC command generation.

Abstract. This paper presents a new method to generate the cam position commands required for manufacturing a cam profile by an open-architecture CNC machine. At first, the junction points of several connected PH quintic curves, as cam segments, are obtained based on the supposed desired follower motion. Consequently, the desired cam curve is represented via a multi-segment C^2 PH quintic curve. After that, a new interpolation algorithm is proposed to generate the position commands required for machining of the cam. The designed cam-follower mechanism is performed for several case studies to evaluate the effectiveness of the employed curve representation and the proposed interpolation algorithm. The simulation results demonstrate that the proposed interpolation algorithm is capable of providing a smooth transition for all regions of the follower motion, and the obtained displacement, velocity, acceleration and jerk profiles match the corresponding desired profiles closely. Therefore, the newly advised interpolation algorithm with a uniform segmentation scheme is not only feasible for generating cam position commands, but also yields a satisfactory performance for the follower motion. Also, the non-uniform rotational segmentation of the cam curve causes the amount of kinematic characteristics of the follower motion to be significantly increased, compared to the corresponding desired profiles.

1. Introduction

Cam-follower mechanisms are commonly used in almost all mechanical systems to transform a desired rotary motion into a rotary/linear motion by direct surface contact. Several investigations have been made into the designing, optimization, operation and production of the cam-follower mechanism [1-13]. The profile of a cam should be designed in such a way that it can produce the specified desired displacement of the follower at each arbitrary cam rotational angle. Furthermore, it should yield the desired kinematic characteristics of the follower motion, such as velocity, acceleration and jerk. Moreover, the cam profile must have the ability to manufacture by means of CNC machines with admissible accuracy. In recent decades, the use of splines as a mathematical representation for a cam profile has become preferred over polynomials because of their versatility, ease of application, and flexibility [9-12]. For instance, Qiu et al. [9] proposed a universal optimal approach consisting of four issues to optimize the uniform B-spline cam curve, while Xiao and Zu [10] employed two types of curve representation in cam profile synthesis, including a general polynomial spline and a B-spline. In this study, the authors applied both a classical optimization technique and a genetic algorithm to solve the cam shape optimization

*. *Corresponding author. Tel.: +98 511 6625046; Fax: +98 511 6627560*
E-mail addresses: jahanpourfr@mshdiau.ac.ir (J. Jahanpour); H.dolat@yahoo.com (H. Dolatabadi)

problem. Although the B-spline curves are flexible and have many nice properties for curve design, they are not able to represent the circular arcs required for the exact dwell of the follower.

The motion of a follower depends on its cam profile. The cam profile is usually designed by combining several connected curves to produce the prescribed follower motion. After designing the cam profile via a CAD representation model, the position commands of the cam profile should be generated to manufacture the cam by a machining process such as milling. Common cam profile representation methods, i.e. polynomial, spline, B-spline, and even Non-Uniform Rational B-Splines (NURBS) yield profiles that require approximation during the interpolation process before they can be imported to the CAD/CAM system [14]. In fact, the position commands required for machining the cam are not generated precisely.

In recent years, a cam profile design has been developed via Pythagorean-Hodograph (PH) curves. These curves, which were first introduced by Farouki and Sakkalis [15] in 1990, are a special family of free-form parametric curves. In contrast with the polynomial/spline, PH curves and their offset admit exact representation within CAD systems, and can also be downloaded to an open-architecture CNC machine without the need of linear/circular G code approximations [16,17]. The fact that the PH curve has a polynomial representation, along with a special algebraic structure, makes it well suited for CNC interpolation algorithms to generate the commands of the tool path presented via the PH curve [18].

One method for designing a cam profile using PH curves is a C^k Hermite PH spline curve constructed by Hermite data of a series of points. This approach always leads to three complex quadratic equations which can be solved by several connected PH curves of degree $4k + 1$ [17,19,20]. In particular, Farouki et al. [17] designed the pitch curve of the cam using two degree-nine PH curves for connecting the circular dwell arcs. Accordingly, the actual cam profile, as the rational curve of degree 17, was found by offsetting the pitch curve at a distance equal to the radius of the roller. In their work, the C^2 Hermite PH spline curve of degree nine was constructed based on the Hermite data obtained from the geometric form of circular arcs in dwell regions. However, the obtained displacement, velocity and acceleration profiles of the follower were presented only for the case of symmetric, and without offset, cam curves, including DRDR (Dwell-Rise-Dwell-Return) phases. The use of the closed C^2 PH quintic spline curve is the other approach to designing a cam pitch curve via PH curves. The C^2 PH quintic spline is associated with given control points, and a knot vector is defined as being the good PH spline interpolant to the nodal points of the cubic B-spline curve, which is specified by the given control polygon and knots [21-23]. In fact, the C^2 PH quintic spline curve includes the PH quintic segments, which are connected with the C^2 of continuity at the points on the cubic B-spline curve corresponding to the specified knot points, $u_0, u_1, ..., u_m$ called nodal points. Because of using the nodal point (and possibly derivatives) of a basic cubic B-spline curve, this approach to designing a cam pitch curve is not easily adopted to accommodate the precisely circular arcs that are required for the exact dwell of the follower [17]. In addition, for the case of closed C^2 PH quintic curves, the first nodal point on the corresponding cubic B-spline curve is specified by the first three control points, which results in mapping in order to transfer that point to the desired point [20]. To cope with the aforementioned difficulty, in this paper, a new approach to design a cam profile via PH curves is proposed. To this end, the cam profile is represented using several connected PH quintic curves with a C^2 continuity condition at the junction points obtained directly from the desired follower motion. In contrast with the C^2 PH spline curves, in which the nodal points are computed according to the control points of a basic cubic B-spline, the junction points are calculated according to the desired follower motion in this paper. This enables the modeling of an exact circular arc in the dwell region of the follower motion. After designing the cam profile using the multi-segment C^2 PH quintic curve, a novel interpolation method to generate position commands required for machining the cam is also devised.

Henceforth, the paper is organized as follows: In Section 2, PH curves are briefly reviewed and the PH quintic curve equations related to the segments between a series of consecutive junction points are described. In Section 3, cam profile representation via a multi-segment C^2 PH quintic curve is presented. Besides, in this section, the novel rotational interpolation method for the designed cam profile is also introduced in order to generate the desired cam position commands. In Section 4, simulation results, such as follower displacement, velocity, acceleration and jerk profiles, obtained from the proposed interpolation algorithm, are presented for two cases of with and without offset cams. Finally, Section 5 concludes the paper.

2. Multi-segment C^2 PH quintic curve

The complex representation for a planar PH curve can be expressed as: $r(\xi) = x(\xi) + iy(\xi)$, where $\xi \in [0, 1]$ is a real parameter [24]. $r(\xi)$ is a PH curve if there exist polynomials, $u(\xi)$ and $v(\xi)$, such that its derivative, i.e. hodograph $r'(\xi) = w^2(\xi)$, satisfies:

$$x'(\xi) = u^2(\xi) - v^2(\xi),$$

$$y'(\xi) = 2u(\xi)v(\xi),$$

$$\sigma(\xi) = u^2(\xi) + v^2(\xi), \quad (1)$$

where $\sigma(\xi(= \sqrt{x'^2(\xi) + y'^2(\xi)} = \left|\frac{d(r(\xi))}{d(\xi)}\right|$ is the rate of change of $r\xi$), with respect to the curve parameter, ξ.

In general, a single PH curve cannot represent complicated open and closed shapes. Nevertheless, the aforementioned difficulty can be circumvented by employing the several connected PH curves [19,20]. Due to the fact that PH quintic curves are most suitable for practical application where flexibility is required [16], a multi-segment C^2 PH quintic curve can be constructed by several connected PH quintic curves with C^2 continuity at the successive junction points, q_0, $q_1, ...,$ q_M. For designing a cam profile in the closed multi-segment C^2 PH quintic curve form, the first- and end-junction points, i.e. q_0 and q_M, should coincide. In this paper, the junction points, $q_0, q_1, ..., q_M$ are computed from the desired follower displacement profile.

Interpolation of the above M junction points begins by writing the hodograph of the PH quintic segment, $r_i(\xi)$, $\xi \in [0, 1]$, of the curve, between points q_{i-1} and q_i. The polynomial $w_i(\xi)$ $u_i(\xi)+iv_i(\xi)$ related to the $r_i(\xi)$ must be quadratic. Expressed in Bernstein form, the corresponding hodograph in complex form is:

$$r'_i(\xi) = [\frac{1}{2}(z_{i-1} + z_i)(1-\xi)^2 + z_i 2(1-\xi)\xi + \frac{1}{2}(z_i + z_{i+1})\xi^2]^2. \quad (2)$$

The continuity conditions for consecutive segments, i and $i+1$, are: $r'_i(1) = r'_{i+1}(0)$, and $r''_i(1) = r''_{i+1}(0)$. Expanding Eq. (2) and substituting it into the interpolation condition integral, $\int_0^1 r'_i(\xi)d\xi = q_i - q_{i-1}$, by talking $r_i(0) = q_{i-1}$ as the integration constant, the following equation will be yielded [21]:

$$f_i(z_{i-1}, z_i, z_{i+1}) = 3z_{i-1}^2 + 27z_i^2 + 3z_{i+1}^2 + z_{i-1}z_{i+1} + 13z_{i-1}z_i + 13z_i z_{i+1} - 60\Delta q_i = 0, \quad (3)$$

where $\Delta q_i = q_i - q_{i-1}$ for $i = 1, ..., M$. However, the first and last equation, i.e. $f_1(z_1, ..., z_M) = 0$ and $f_M(z_1, ..., z_M) = 0$, must be modified or additional equations must be introduced through the end conditions. For the closed multi-segment C^2 PH quintic curves, end conditions: $q_M = q_0$, $r'_M(1) = r'_1(0)$, and $r''_M(1) = r''_1(0)$ should be satisfied. To this end, Eq. (2) is replaced by the following relations [21]:

$$r'_1(\xi) = [\frac{1}{2}(\pm z_M + z_1)(1-\xi)^2 + z_1 2(1-\xi)\xi + \frac{1}{2}(z_1 + z_2)\xi^2]^2,$$

$$r'_M(\xi) = [\frac{1}{2}(z_{M-1} + z_M)(1-\xi)^2 + z_M 2(1-\xi)\xi + \frac{1}{2}(z_M \pm z_1)\xi^2]^2. \quad (4)$$

Therefore, the first and last equations of the system described by Eq. (3) become:

$$f_1(z_1, ..., z_M) = 3z_M^2 + 27z_1^2 + 3z_2^2 \pm z_M z_2 \pm 13z_M z_1 + 13z_1 z_2 - 60\Delta q_1 = 0,$$

$$f_M(z_1, ..., z_M) = 3z_{M-1}^2 + 27z_M^2 + 3z_1^2 \pm z_{M-1}z_1 + 13z_{M-1}z_M \pm 13z_M z_1 - 60\Delta q_M = 0. \quad (5)$$

In order to solve the system equation described by Eq. (3) with end conditions, i.e. Eq. (5), numerical methods should be used. The Newton-Raphson iteration algorithm can be employed to compute unknowns, $z_1, ..., z_M$ appropriate starting approximation. In this paper, the starting approximation is calculated using the method developed in [21]. Further details on using the Newton-Raphson iteration method and the starting approximation can be found in [21-23]. After solving the aforementioned system of equations, the hodographs of the PH quintic segment are found by Eqs. (2) and (4). Consequently, the multi-segment C^2 PH quintic curve is obtained by integrating these hodographs by taking $r_i(0) = q_{i-1}$ as the integration constants, i.e.:

$$r_i(\xi) = \int_0^\xi r'_i(\zeta)d\zeta + q_{i-1}. \quad (6)$$

3. CNC command generation of the cam profile represented via multi-segment C^2 PH quintic curve

As mentioned, the junction points, q_0, $q_1, ...,$ q_M, are required for accomplishing the PH quintic segment, i.e. Eqs. (3)-(6), to obtain the multi-segment C^2 PH quintic curve as the representation of the cam profile. In this section, at first, the procedure of obtaining the junction points is presented. Then, the rotational multi-segment C^2 PH quintic curve interpolant is illustrated to generate the desired cam position commands.

3.1. Cam profile representation via multi-segment C^2 PH quintic curve

A few analytical functions are used to describe the rise and return parts of the displacement diagram while meeting the smoothness conditions. These are cycloid, harmonic, and polynomial functions. In this paper, the cycloidal motion, as the desired follower displacement, is taken into consideration. Besides, due to the fact

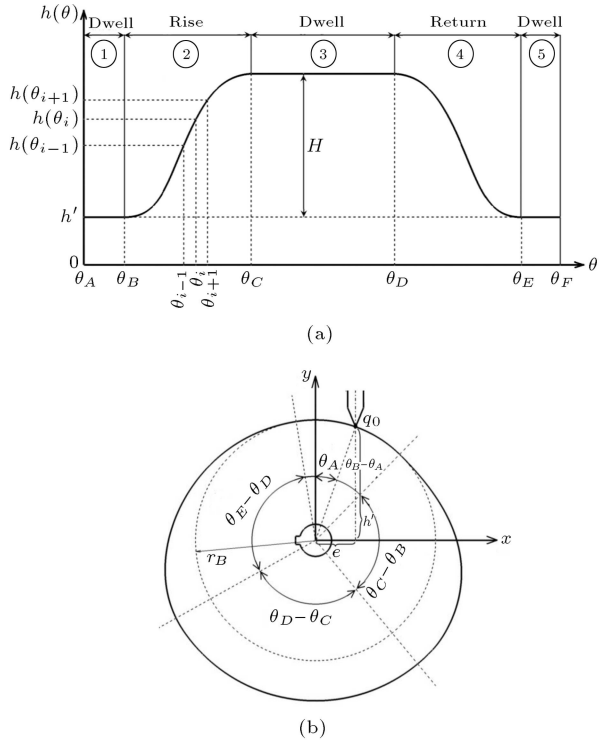

Figure 1. A cam-follower mechanism with cycloidal motion in the rise/return region: (a) DRDRD knife-edge follower displacement diagram; and (b) cam parameters.

that the cam shape is an offset to the pitch curve at a distance equal to the radius of the roller, for the case of a cam-follower mechanism with a roller follower, the knife edge follower shape is used in this paper. Nevertheless, the method is extensible to the other types of follower shape, along with the other desired follower displacement.

In general, the desired displacement profile of the follower shown in Figure 1(a) has a cycle of DRDRD (Dwell-Rise-Dwell-Return-Dwell) motion and is cycloidal in the rise and return regions. According to Figure 1, θ_B, θ_C, θ_D and θ_E are the angles corresponding to the beginning of the rise, the middle dwell, the return, and the last dwell regions, respectively. Also, $\theta_F = 2\pi + \theta_A$ is the angle corresponding to the termination point of complete cam rotation and $h_(\theta)$ is the desired follower displacement, with respect to the cam rotation angle, $\theta \in [\theta_A, \theta_F]$. Furthermore, H is the maximum rise of the follower and h' is the minimum displacement of the follower. The basic circle is also depicted in Figure 1(b) as a dotted circle.

θ_A is the angle corresponding to $h(\theta) = h'$ at the beginning of the first dwell region of the follower. Accordingly, the follower motion is started from where it is related to the angle, $\theta = \theta_A$. The amount of this angle can be computed by the following relation:

$$\theta_A = \sin^{-1}\left(\frac{e}{r_B}\right), \; r_B = \sqrt{(h'^2 + e^2)}. \tag{7}$$

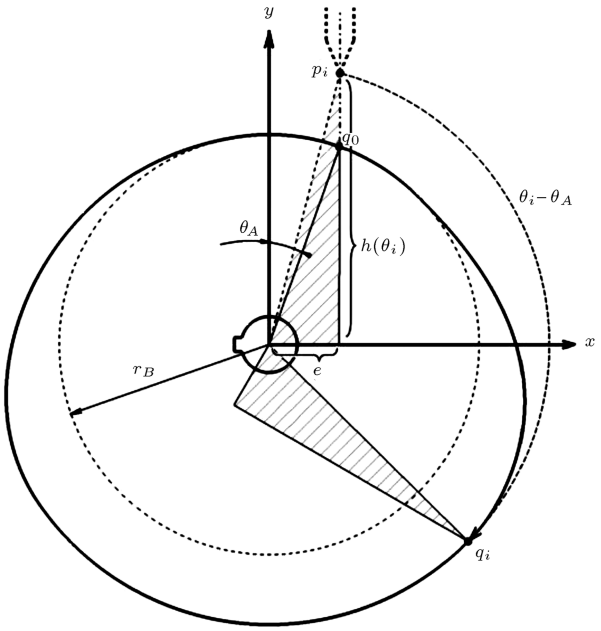

Figure 2. Junction points location on the multi-segment C^2 PH quintic cam curve.

In the above relation, e and r_B are the cam offset and the radius of the basis circle, respectively (see Figure 1(b)).

The relation of the desired follower displacement, $h(\theta)$ and the cam rotation angle, θ, using cycloidal motion, can be expressed as follows [17]:

$$h(\theta) = h' + \frac{H}{2\pi}\left(2\pi\frac{\theta}{\beta} - \sin 2\pi\frac{\theta}{\beta}\right), \tag{8}$$

where, β is equal to $\beta = \beta_{ri} = \theta_C - \theta_B$ in the rise region, and $\beta = \beta_{re} = \theta_E - \theta_D$ in the return region.

The follower velocity, the follower acceleration and the follower jerk can be obtained by differentiating the above relation and the maximum of these kinematic characteristics can be easily computed, consequently.

The start point of the dwell region located under the follower corresponding to the angle θ_A is on the basis circle as well as on the cam curve. This point shown in Figure 2 is assumed as the first junction point, i.e. q_0. According to Figure 2 and the desired follower displacement diagram shown in Figure 1(a), the position of point located under the follower corresponding to angle θ_i can be expressed as:

$$p_i = \begin{bmatrix} e \\ h(\theta_i) \end{bmatrix}, \; i = 1, ... \tag{9}$$

Therefore, the position of junction point, q_i, on the cam curve can be calculated as follows:

$$q_i = \begin{bmatrix} \cos(\theta_i - \theta_A) & \sin(\theta_i - \theta_A) \\ -\sin(\theta_i - \theta_A) & \cos(\theta_i - \theta_A) \end{bmatrix} \begin{bmatrix} e \\ h(\theta_i) \end{bmatrix}, \; i = 0, 1, ..., M. \tag{10}$$

As can be seen in Eq. (10), the position of junction point, q_i, corresponding to the angle θ_i on the cam, is evaluated according to the supposed desired follower displacement of $h(\theta)|_{\theta=\theta_i} = h(\theta_i)$.

The number of junction points, q_i, and the segmentation type for angles θ_i have a significant role in creating a smooth cam profile. In this paper, the cam profile is designed in the form of a multi-segment C^2 PH quintic curve using uniform segmentation for angles, θ_i, and the effect of non-uniform segmentation is also analyzed. According to Figure 1(a), for the case of uniform segmentations through all regions of cam motion, the angle related to junction point q_i is computed as follows:

$$\theta_i = (\theta_F - \theta_A)\frac{i}{M} = \frac{2\pi i}{M}. \tag{11}$$

The number of segmentations for a complete cam rotation cycle, i.e. M, is specified for maintaining deviation of the obtained actual follower displacement from the desired follower displacement within the allowable tolerance limit, ε_{all}.

3.2. The rotational multi-segment C^2 PH quintic curve interpolant

In the following, a new algorithm for rotational interpolating the multi-segment C^2 PH quintic curve, as the cam profile, is introduced in order to generate the desired cam position commands related to cam rotation with constant angular velocity of w.

The cam-follower mechanism, along with the ith PH quintic segment, curve described by Eq. (6), between two junction points, q_{i-1} and q_i, corresponding to the consecutive angles, θ_{i-1} and θ_i, are shown in Figure 3.

$\vec{r}_i(\xi_{i,k})$ is the position vector of point $R_{i,k}$ on the ith PH quintic segment curve corresponding to parameter $\xi_{i,k} \in [0,1]$ for the ith PH quintic segment (see Figure 3(b)). $\vec{r}_i(\xi_{i,k})$ contains the real and imaginary parts in the x and y directions, respectively, i.e.:

$$r_{i,x}(\xi_{i,k}) = \text{Real } (r_i(\xi_{i,k}),$$

$$r_{i,y}(\xi_{i,k}) = \text{Image } (r_i(\xi_{i,k})). \tag{12}$$

The curve parameter, $\xi_{i,k}$, is evaluated, such that point $R_{i,k}$ can be located under the follower after rotation of the cam by the amount of $\theta_{i,k}$. Therefore, as depicted in Figure 3(a), the horizontal component of position vector $\vec{r}_i(\xi_{i,k})$ should be equal to the offset after rotating the cam by $\theta_{i,k}$. That is:

$$e = r_{i,x}(\xi_{i,k})\cos\theta_{i,k} - r_{i,y}(\xi_{i,k})\sin\theta_{i,k},$$

$$\text{for } i = 1, ..., M, \tag{13}$$

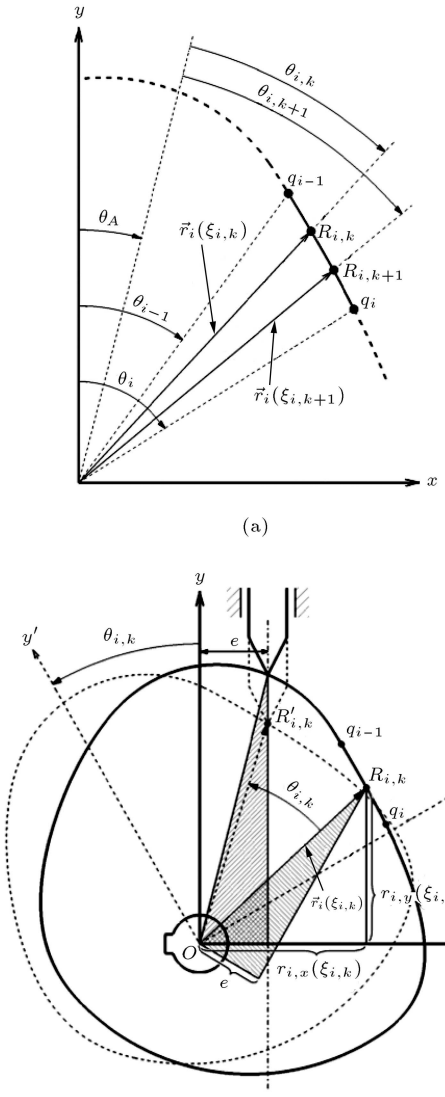

Figure 3. Cam-follower mechanism with rotation angle of $\theta_{i,k}$: (a) Points location after rotation; and (b) ith segment of the multi-segment C^2 PH quintic curve.

where $\theta_{i,k} = (\theta_{i-1} - \theta_A) + k\Delta\varphi$ and $\Delta\varphi = \omega\Delta t$ is the interpolation angle corresponding to the sampling period of Δt.

The sequence of parameter values, $\xi_{i,1} = 0$, $\xi_{i,2}, ..., \xi_{i,N} = 1$, is computed by Eq. (13). This equation has a unique real root, $\xi_{i,k}$, which can be determined using the Newton-Raphson method, as follows after r iterations:

$$\xi_{i,k}^{r} = \xi_{i,k}^{(r-1)} - \frac{r_{i,x}(\xi_{i,k})\cos\theta_{i,k} - r_{i,y}(\xi_{i,k})\sin\theta_{i,k} - e}{r'_{i,x}(\xi_{i,k})\cos\theta_{i,k} - r'_{i,y}(\xi_{i,k})\sin\theta_{i,k}}$$

$$\text{for } i = 1, ..., M. \tag{14}$$

An initial approximation for each iteration can be considered as $\xi_{i,k}^{(0)} = \xi_{i,k-1}$. The desired cam position commands in the x and y directions, i.e. $X_{\text{com}}(i,k)$ and

$Y_{\text{com}}(i,k)$, respectively, are calculated by substituting computed $\xi_{i,k}$ (from Eq. (14)) in Eqs. (6) and (12), as follows:

$$X_{\text{com}}(i,k) = \text{Real}\,(r_i(\xi_{i,k})) = \text{Real}\left\{\int_0^{\xi_{i,k}} r_i'(\zeta)d\zeta + q_{i-1}\right\},$$

$$Y_{\text{com}}(i,k) = \text{Image}(r_i(\xi_{i,k})) = \text{Image}\left\{\int_0^{\xi_{i,k}} r_i'(\zeta)d\zeta + q_{i-1}\right\}. \quad (15)$$

The above commands can be used in an open-architecture CNC machine for manufacturing the cam profile curve.

4. Simulations

In order to illustrate the efficiency of using the multi-segment C^2 PH quintic curve in representation of a cam profile, and also the feasibility of the proposed rotational interpolation algorithm, three cases are illustrated in the simulations described in the following subsection.

4.1. Case studies

The first and second case studies are considered for cams without an offset, i.e. $e = 0$, and with offset of $e = 10$ (mm), respectively.

As mentioned before, the number of cam segments, i.e. M, is chosen to keep the deviation displacement error within the specified tolerance limit, ε_{all}.

For these cases, the cam profile curve is divided into $M-60$ uniform rotational segments of θ_i thorough the all regions of the cam motion, which results in $q_0,\ q_1,\ldots,\ q_{60} = q_0$ as points corresponding to angles $\theta_i = i^*\pi/30$ (rad).

The third case is adopted for the cam with an offset of $e = 10$ (mm). In this case, cam profile is divided into $M = 64$ rotational segments, including 24 segments with equal rotational segmentation of $i^*\pi/36$ (rad) for the dwell regions, and 40 segments with equal rotational segmentation of $i^*\pi/30$ (rad) for the rise and return regions of the follower motion.

4.2. Simulation results

The cam-follower mechanism parameters used in the simulations are given in Table 1. Also, the sampling period time for rotational interpolation of the multi-segment C^2 PH quintic curve to compute the cam position commands is equal to $\Delta t = 1$ (ms) in all simulations. Furthermore, the maximum allowable displacement error between the actual follower motion and the desired follower displacement, i.e. ε_{all}, is assumed as a small amount of $\varepsilon_{\text{all}} = 0.2$ (μm).

Table 1. The cam-follower mechanism parameters.

First dwell angle of cam: $\theta_B - \theta_A$ (deg)	30
Rise angle of cam: $\beta_{ri} = \theta_c - \theta_B$ (deg)	120
Middle dwell angle of cam: $\theta_D - \theta_C$ (deg)	60
Return angle of cam: $\beta_{re} = \theta_E - \theta_D$ (deg)	120
Last dwell angle of cam: $\theta_F - \theta_E$ (deg)	30
Minimum displacement of follower: h' (mm)	20
Maximum rise of follower: H (mm)	20
Cam angular velocity: ω (rpm)	60

With the cam-follower mechanism parameters listed in Table 1, the maximum amounts of velocity, acceleration and jerk for the desired cycloidal follower motion are computed as 120 (mm/s), 1,130.9 (mm/s^2) and 21,318.3 (mm/s^3), respectively.

The simulation results for the first case, i.e. $e = 0$, and uniform segmentation with $M = 60$ are shown in Figure 4. Figure 4(a) shows the cam profile, including 60 segments of PH quintic curves with a continuity of C^2 at the junction points computed by Eq. (10). Also, the inset shows a part of the generated cam position commands computed by the proposed interpolation algorithm. The basis circle is also shown in Figure 4(a). The angle related to the first dwell region, i.e. θ_A, is equal to zero for this case. Figure 4(b) to (e) is the actual displacement, velocity, acceleration and jerk profiles of the follower, with respect to cam rotation angle, $\theta_{i,k}$, respectively. In these figures, the kinematic characteristics of the desired motion are also depicted. In Figure 4(b), it can be observed that the obtained follower displacement profile employing cam representation via multi-segment C^2 PH quintic curves with the proposed rotational interpolation algorithm, is able to achieve the desired cycloidal motion. As can be seen in Figure 4(c) to (e), the obtained velocity, acceleration and jerk profiles have acceptable accuracy compared to the desired cycloidal motion. The maximum amounts of actual velocity, acceleration and jerk are equal to 120 (mm/s), 1,141 (mm/s^2) and 23,200 (mm/s^3), respectively. These values are close to the desired kinematic characteristics of cycloidal motion. It can be found that maximum actual acceleration (jerk) is increased by a small amount of 0.88% (8.82%) with respect to the maximum desired acceleration (jerk), while maximum actual velocity is equal to its maximum desired value.

The Maximum error between the actual follower displacement and the desired follower displacement is a small amount of 0.14 (μm) Figure 5. This maximum error is related to the rise/return region of the follower motion. According to Figure 5, it is found that the smaller deviation errors of the actual

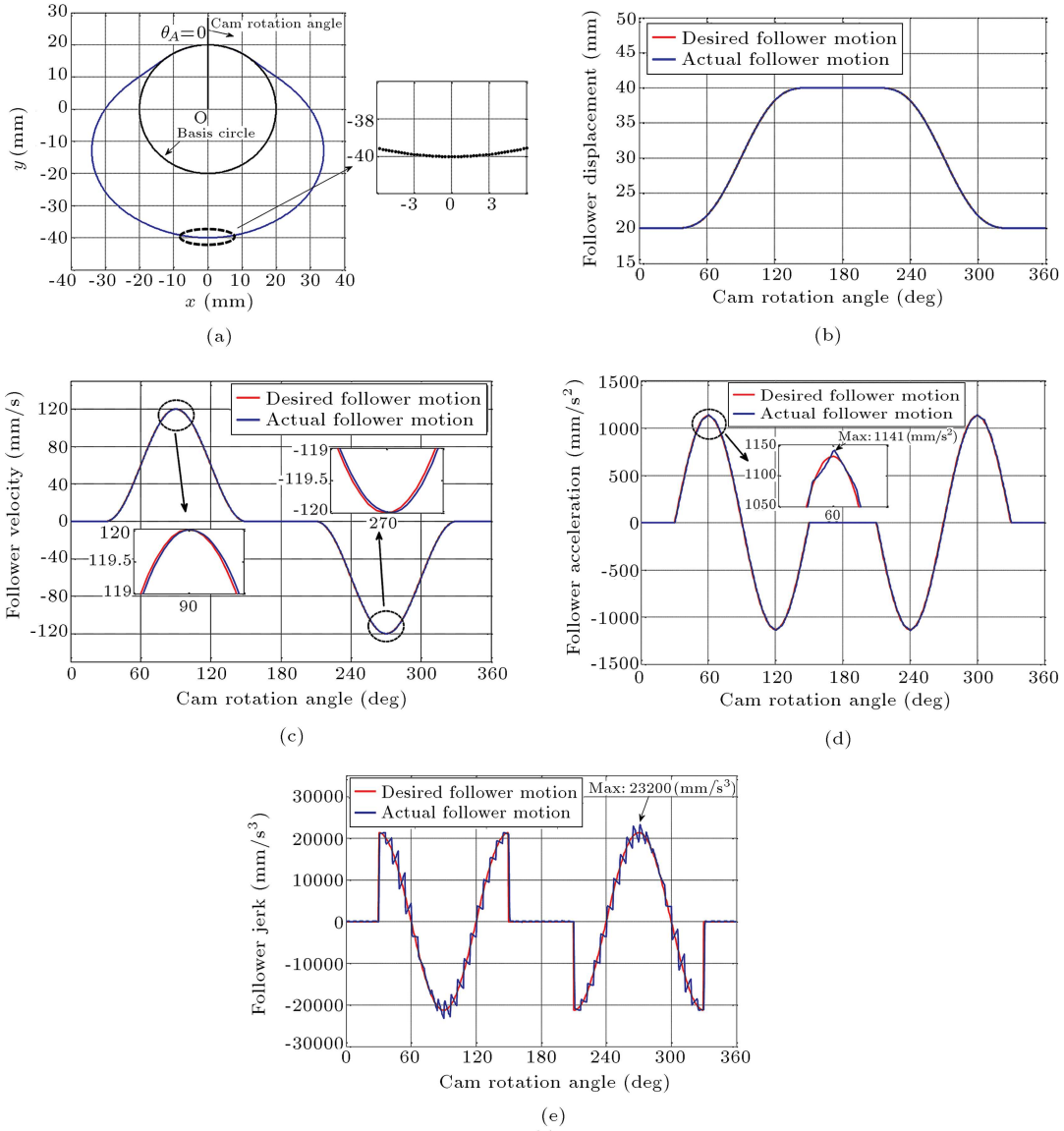

Figure 4. Kinematic characteristics of the actual/desired follower motion for the case of $e = 0$ (mm) and uniform segmentation with $M = 60$: (a) Designed cam profile via multi-segment C^2 PH quintic curve; (b) displacement profile; (c) velocity profile; (d) acceleration profile; and (e) jerk profile.

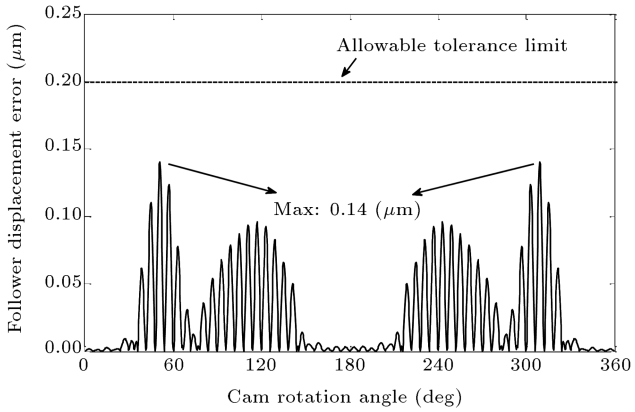

Figure 5. Displacement error from the desired follower motion for the case of $e = 0$ (mm) and uniform segmentation with $M = 60$.

follower displacement from the desired values occur at the portions of motion in the dwell regions. Therefore, the proposed multi-segment C^2 PH quintic curve, along with its interpolation algorithm, is capable of constructing precise circular arcs that are required for the exact dwell of the follower. The simulation results are summarized in Table 2.

Figure 6 shows the results for the second case, in which the cam has an offset of 10 (mm). Figure 6(a) shows the designed cam profile via a multi-segment C^2 PH quintic curve, along with the basis circle of the cam. Furthermore, the inset shows a part of the generated cam position commands computed by the proposed interpolation algorithm. The angle of the first dwell region computed by Eq. (7) is $\theta_A = 26.565°$. For this case, i.e. $e = 10$ (mm) and uniform segmen-

Table 2. Simulation results for the follower motion.

Cam offset and segmentation type	Maximum deviation error (μm)	Maximum velocity (mm/s)	Maximum acceleration (mm/s^2)	Maximum jerk (mm/s^3)
Case 1: e=0 (mm) and uniform segmentation with $M = 60$	0.14	120	1.141	23.200
Case 2: e=10 (mm) and uniform segmentation with $M = 60$	0.15	120	1.144	23.680
Case 3: e=10 (mm) and non-uniform segmentation with $M = 64$	3.9	120	1.143	62.243

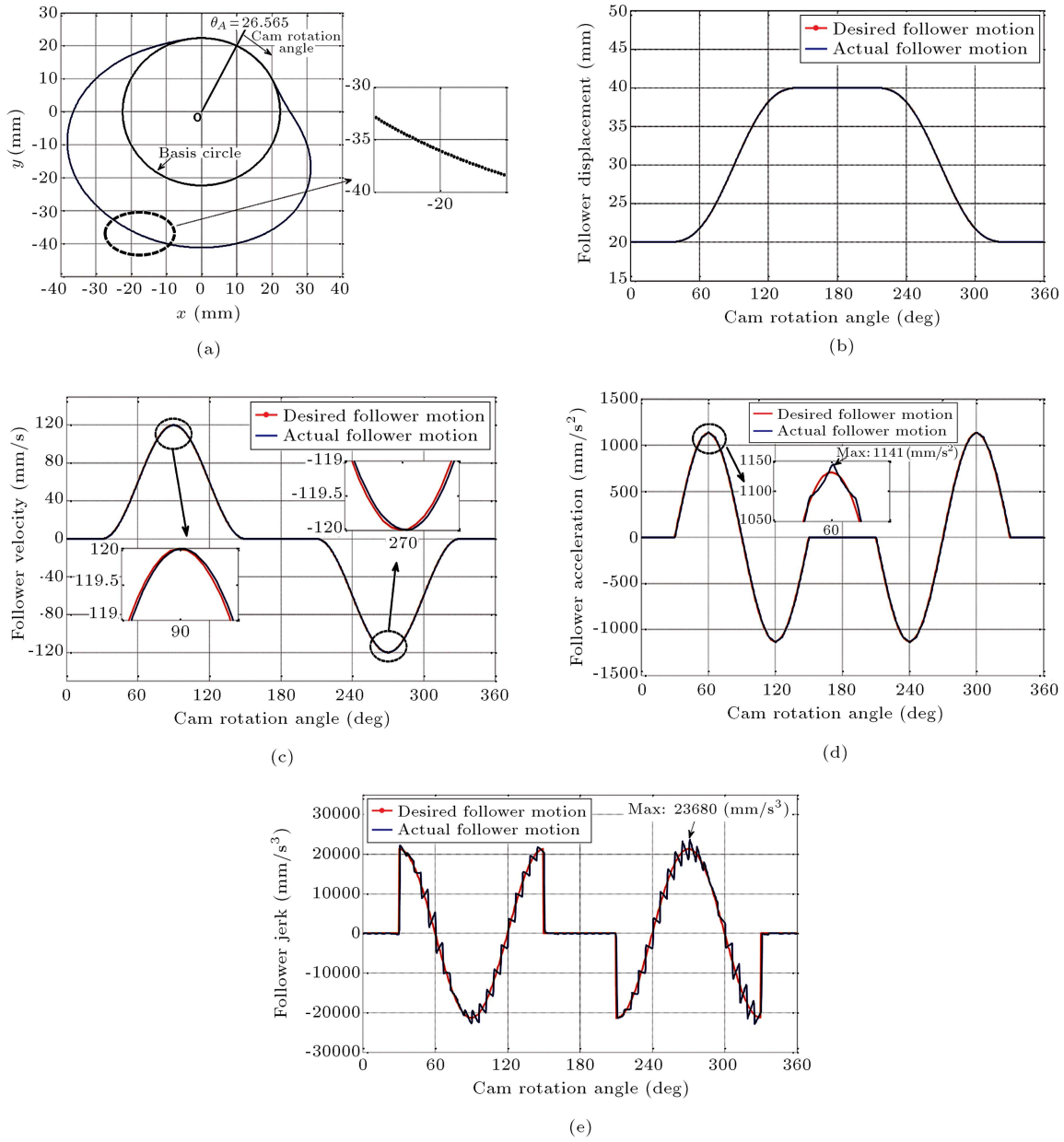

Figure 6. Kinematic characteristics of the actual/desired follower motion for the case of $e = 10$ (mm) and uniform segmentation with $M = 60$: (a) Designed cam profile via multi-segment C^2 PH quintic curve; (b) displacement profile; (c) velocity profile; (d) acceleration profile; and (e) jerk profile.

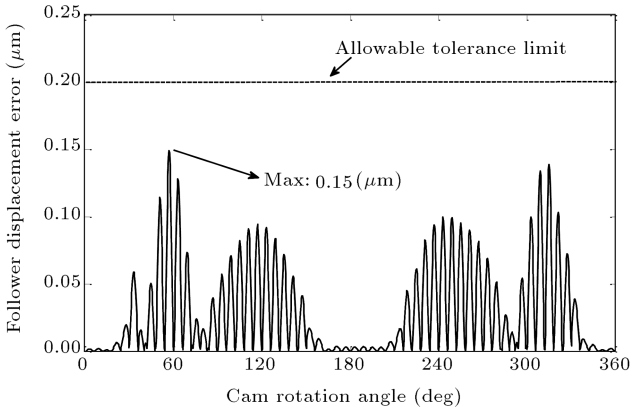

Figure 7. Displacement error from the desired follower motion for the case of $e = 10$ (mm) and uniform segmentation with $M = 60$.

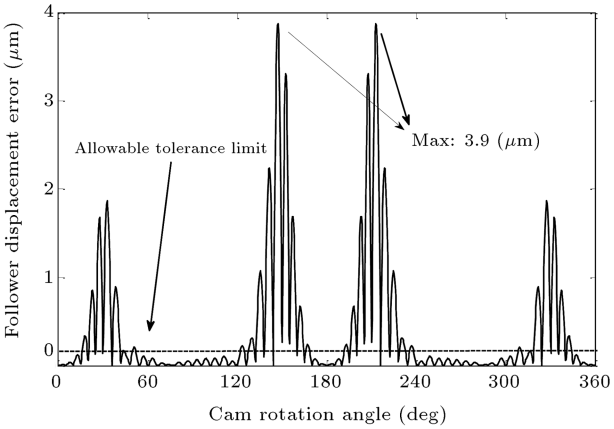

Figure 8. Displacement error from the desired follower motion for the case of $e = 10$ (mm) and non-uniform segmentation with $M = 64$.

tation with $M = 60$, the actual displacement, velocity, acceleration and jerk profiles of the follower, with respect to cam rotation angle, $\theta_{i,k}$, are shown in Figure 6(b) to (e), respectively. The kinematic characteristics of the desired cycloidal motion are also illustrated. As can be seen in Figure 6(b) to (e), the obtained displacement, velocity, acceleration and jerk profiles match the corresponding desired profiles closely (see also Table 2). Considering Figure 7, it has been observed that the maximum deviation error of the follower displacement from the cycloidal displacement is about 0.15(μm), which is within in the tight tolerance limit of $\varepsilon_{\text{all}} = 0.2(\mu\text{m})$. For this case, the maximum deviation error is also related to the rise/return region, while the smaller deviation errors of the actual follower displacement from the desired values occur in the dwell regions. The achieved small deviation errors not only demonstrate satisfactory uniform rotational segmentation performance, but also create the precisely circular arcs for dwell regions of the motion.

As reported in Table 2, the actual kinematic characteristics are also close to their desired values for this case. Maximum actual acceleration (jerk) is increased by a small amount of 1.15% (11.07%), with respect to the maximum desired acceleration (jerk), while maximum actual velocity is equal to its maximum desired value.

In order to investigate the effect of non-uniform segmentation for θ_i characteristics of the motion, the third case is explained in the following. This case includes 64 PH quintic segments compared to 60 PH quintic segments used in the second case study. The simulation results for the third case, i.e. $e = 10$ (mm), and non-uniform segmentation with $M = 64$, are also presented in Table 2. Although maximum actual velocity and acceleration are close to their maximum desired values, maximum actual jerk is increased up to 191.9%, with respect to maximum desired jerk. Also, it is observed that the maximum deviation error of the follower displacement from the desired displacement is about 3.9 (μm), that exceeds the allowable tolerance limit, ε_{all} (see Figure 8). This maximum deviation error is related to changing the follower motion from the rise region to the dwell region. As can be seen in Figure 8, the amount of deviation error is increased significantly, in spite of increasing the number of C^2 PH quintic segments for constructing the cam profile. In fact, the non-uniform segmentations for θ_i thorough the all regions of cam motion, i.e. dwell-rise-dwell-return-dwell regions, cause the amount of deviation error to significantly increase.

The simulation results for the third case indicate that the rotational segmentation scheme has a significant effect on the kinematic characteristics of the follower motion.

5. Conclusions

This paper has introduced a new interpolation method to generate the position commands required for machining the cam profile represented via a multi-segment C^2 PH quintic curve. Using specifications of the cam-follower mechanism, such as the cam offset along with the desired follower displacement diagram, the junction points of the connected PH quintic segments are specified with respect to cam rotation angle. The number of junction points is selected for maintaining the deviation error of the actual follower displacement, and the desired one within a certain limit. The simulation results for two cases of cam-follower mechanism, with offset and without offset, confirm that the proposed multi-segment C^2 PH quintic curve with uniform segmentation is capable of constructing precisely circular arcs for dwell regions of the follower motion, this is the main advantage over the other cam design methods based on PH-spline curves. Also,

non-uniform cam segmentation through all regions of motion causes the amount of the deviation error from the desired follower displacement to be significantly increased. As can be seen in the simulation results, the proposed interpolation algorithm yields satisfactory kinematic characteristics for follower motion with tight deviation error. Therefore, the cam position commands generated by the newly proposed interpolation algorithm provide a smooth transition for different regions of follower motion.

References

1. Purohit, R. and Sagar, R. "Fabrication of a cam using metal matrix composites", *Int J. Adv. Manuf. Technol.*, **17**(9), pp. 644-648 (2001).
2. Chen, J.H. and Wu, Y.J. "Research in non-equalization machining method for spatial cam", *J. Zhejiang Univ. Sci. A.*, **9**(9), pp. 1258-1263 (2008).
3. Fisette, P., Péterkenne, J.M., Vaneghem, B. and Samin, J.C. "A multibody loop constraints approach for modeling cam/follower devices", *Nonlinear Dyn.*, **22**(4), pp. 335-359 (2000).
4. Yin, G.F., Tian, G.Y. and Taylor, D. "A web-based remote cooperative design for spatial cam", *Int. J. Adv. Manuf. Technol.*, **20**(8), pp. 557-563 (2002).
5. Zhang, Y. and Shin, J.H. "A computational approach to profile generation of planar cam mechanisms", *J. Mech. Design*, **126**(1), pp. 183-188 (2004).
6. Nguyena, V.T. and Kim, D.J. "Flexible cam profile synthesis method using smoothing spline curves", *Mech. Mach. Theory*, **42**(7), pp. 825-838 (2007).
7. Lampinen, J. "Cam shape optimisation by genetic algorithm", *Comp. Aided Des.*, **35**(8), pp. 727-737 (2003).
8. Bouzakis, K.D., Mitsi, S. and Tsiafis, J. "Computer aided optimum design and NC milling of planar cam mechanisms", *Int. J. Mach. Tools Manufact.*, **37**(8), pp. 1131-1142 (1997).
9. Qiu, H., Lin, C.J., Li, Z.Y., Ozaki, H., Wang, J. and Yue, Y. "A universal optimal approach to cam curve design and its applications", *Mech. Mach. Theory*, **40**(6), pp. 669-692 (2005).
10. Xiao, H. and Zu, J.W. "Cam profile optimization for a new cam drive", *J. Mech. Sci. Technol.*, **23**(10), pp. 2592-2602 (2009).
11. Naskar, T.K. and Mishra, R. " Introduction of control points in B-splines for synthesis of ping finite optimized cam motion program", *J. Mech. Sci. Technol.*, **26**(2), pp. 489-494 (2012).
12. Sateesh, N., Rao, C.S.P. and Janardhan Reddy, T.A. "Optimisation of cam-follower motion using B-splines", *Int. J. Comp. Integ. Manuf.*, **22**(6) pp. 515-523 (2009).
13. Chiu, H.C. and Lin, T.R. "A novel reverse measurement and manufacturing of conjugate cams in a diesel engine", *Int. J. Adv. Manuf. Technol.*, **26**(1-2) pp. 41-46 (2005).
14. Farouki, R.T. and Tsai Y.F. "Exact Taylor series coefficients for variable-feedrate CNC curve interpolators", *Comput. Aided Geom. Des.*, **33**(2), pp. 155-165 (2001).
15. Farouki, R.T. and Sakkalis, T. "Pythagorean hodographs", *IBM J. Res. Dev.*, **34**(5) pp. 736-752 (1990).
16. Farouki, R.T., Manjunathaiah, J. and Yuan, G.F. "G codes for the specification of pythagorean-hodograph tool paths and associated feedrate functions on open-architecture CNC machines", *Int. J. Mach. Tool Manufact.*, **39**(1) pp. 123-142 (1997).
17. Farouki, R.T., Manjunathaiah, J. and Jee, S. "Design of rational cam profiles with pythagorean-hodograph curves", *Mech. Mach. Theory*, **33**(6), pp. 669-682 (1998).
18. Farouki, R.T., Tsai, Y.F. and Yuan, G.F. "Contour machining of free-form surfaces with real-time PH curve CNC interpolators", *Comput. Aided Geom. Des.*, **16**, pp. 61-76 (1999).
19. Sir, Z. and Juttler, B. "Constructing acceleration continuous tool paths using Pythagorean Hodograph curves", *Mech. Mach. Theory*, **40**(11), pp. 1258-1272 (2005).
20. Jahanpour, J., Tsai, M-C. and Cheng, M.Y. "High speed contouring control with NURBS-based C^2 PH spline curves", *Int. J. Adv. Manuf. Technol.*, **49**(5-8), pp. 663-674 (2010).
21. Pelosi, F., Sampoli, M.L., Farouki, R.T. and Manni, C. "A control polygon scheme for design of planar C^2 PH quintic spline curves", *Comput. Aided. Geom. Des.*, **24**(1), pp. 28-52 (2007).
22. Farouki, R.T., Kuspa, B.K., Manni, C. and Sestini, A. "Efficient solution of the complex quadratic tridiagonal system for C^2 PH quintic splines", *Numer Algor.*, **27**(1), pp. 35-60 (2001).
23. Jahanpour, J. "High speed contouring enhanced with C^2 PH quintic spline curves", *Scientia Iranica, Trans. B: Mech. Eng.*, **19**(2), pp. 311-319 (2012).
24. Moon, H.P., Farouki, R.T. and Choi, H.I. "Construction and shape analysis of PH quintic hermite interpolants", *Comput. Aided. Geom. Des.*, **18**(2) pp. 93-115 (2001).

Biographies

Javad Jahanpour received a BS degree in Mechanical Engineering from Ferdowsi University of Mashhad,

Iran, an MS degree in Applied Mechanical Engineering from Isfahan University of Technology, Isfahan, Iran, and a PhD degree, with first class honours, in Mechanical Engineering, in 2008, from Ferdowsi University of Mashhad, Iran. He is currently Assistant Professor in the Mechanical Engineering Department at the Islamic Azad University of Mashhad, Iran. His research interests include trajectory generation and control motion problem with applications in robotics, vibration and CAD/CAM systems.

Hossein Dolatabadi received his MS degree in Applied Mechanical Engineering from Islamic Azad University of Mashhad (IAUM), Iran, in 2011. His research interests include control motion problem in mechanisms and CAD/CAM systems.